

Inhibition of Dipeptidyl Peptidase IV (DPP-IV) with Sitagliptin (MK0431) Prolongs Islet Graft Survival in Streptozotocin (STZ)-induced Diabetic Mice

Su-Jin Kim¹, Cuilan Nian¹, Doris J. Doudet² and Christopher H. S. McIntosh^{1#}

From the Department of Cellular & Physiological Sciences and the Diabetes Research Group, Life Sciences Institute¹, University of British Columbia, 2350 Health Sciences Mall, the Department of Medicine², Vancouver, B.C., V6T 1Z3, Canada.

Corresponding Author:

Dr. C.H.S. McIntosh
Department of Cellular & Physiological Sciences,
The Diabetes Research Group, Life Sciences Institute,
University of British Columbia
2350 Health Sciences Mall
Vancouver, B.C., V6T 1Z3
mcintosh@interchange.ubc.ca

Received for publication 19 November 2007 and accepted in revised form 19 February 2008.

Additional information for this article can be found in an online appendix at
<http://diabetes.diabetesjournals.org>.

ABSTRACT

Objective: Dipeptidyl peptidase-4 (DPP-IV) inhibitors have been introduced as therapeutics for type 2 diabetes (T2DM). They partially act by blocking degradation of the incretin hormones glucagon-like peptide-1 (GLP-1) and glucose-dependent insulintropic polypeptide (GIP), thus increasing circulating levels of active hormones. In addition to their insulintropic actions, GLP-1 and GIP also promote β -cell proliferation and survival, and DPP-IV inhibitors exert similar effects in rodent T2DM models. The study objective was to establish whether DPP-IV inhibitor treatment prolonged survival of transplanted islets and to determine whether positron emission tomography (PET) was appropriate for quantifying the effect of inhibition on islet mass.

Research Design and Methods: Effects of the DPP-IV inhibitor MK0431 (sitagliptin) on glycemic control and functional islet mass in a streptozotocin (STZ)-induced type 1 diabetes (T1DM) mouse model was determined with metabolic studies and microPET imaging.

Results: The T1DM mouse model exhibited elevated plasma DPP-IV levels that were substantially inhibited in mice on an MK0431- diet. Residual β -cell mass was extremely low in STZ-diabetic mice and, although active GLP-1 levels were increased by the MK0431 diet, there were no significant effects on glycemic control. Following islet transplantation, mice fed normal diet rapidly lost their ability to regulate blood glucose, reflecting the sub-optimal islet transplant. By contrast, the MK0431 group fully regulated blood glucose throughout the study and PET imaging demonstrated a profound protective effect of MK0431 on islet graft size.

Conclusions: Treatment with DPP-IV inhibitor can prolong islet graft retention in an animal model of T1DM.

ABBREVIATIONS. DPP-IV, dipeptidyl peptidase IV; GIP, glucose-dependent insulintropic polypeptide; GLP-1, glucagons-like peptide-1; STZ, streptozotocin; T1DM, Type 1 diabetes; T2DM, Type 2 diabetes; PET, positron emission tomography; NCD, normal chow diet; HSV1-Sr39TK, mutant form of herpes simplex virus 1 thymidine kinase; [¹⁸F]FHBG, 9-(4-[¹⁸F]-Fluoro-3-hydroxymethylbutyl)-guanine; TACs, time activity curves; MAP, maximum *a posteriori*; ROI, region of interest; m.o.i, multiplicity of infection; *HSV1-Sr39TK*, mutant form of herpes simplex virus 1 thymidine kinase; rAD-TK, recombinant adenovirus expressing *HSV1-Sr39TK*; IPGTT, intraperitoneal glucose tolerance test; GSIS, glucose-stimulated insulin secretion; ANOVA, analysis of variance; SEM, standard errors of the mean; AUC, area under the curve.

Over the past few years significant progress has been made in the development of protocols for transplantation of human pancreatic islets in type 1 diabetes (T1DM) (1). However, in recent studies only 67 % (2) and 10 % (3) of transplant recipients were insulin-independent at the end of 1 year and 5 years, respectively. Additionally, at least two donor pancreases are generally needed per transplantation (4), due to the loss of viable islets both during isolation and following transplantation. The causes of post-transplant islet loss are multiple and probably include deficiencies in survival factors (5), altered islet vasculature resulting in deficient nutrient and oxygen delivery (6, 7) inflammation and immune-mediated destruction and the toxic effects of immunosuppressive agents (7). There is therefore considerable interest in developing methods for improving the viability of isolated islets and prolonging their survival. Glucose-dependent insulinotropic polypeptide (GIP) and glucagon-like peptide-1 (GLP-1) are gastrointestinal hormones that potentiate glucose-stimulated insulin secretion, i.e. they are classified as incretins. Additionally, they both stimulate insulin biosynthesis and stimulate proliferation of the β cell, while inhibiting apoptosis (8-12). Termination of the actions of both GIP and GLP-1 is performed by dipeptidyl peptidase IV (DPP-IV; CD26) (13-15) an integral membrane glycoprotein that is also present in soluble form in blood plasma. DPP-IV acts on oligopeptides by selectively removing N-terminal dipeptides (16, 17). Although GIP and GLP-1 exert powerful pro-survival actions on the islet, their short half-lives in the circulation limit their potential usefulness as therapeutic agents. Members of two classes of compounds that circumvent this problem have recently been approved by the FDA: the DPP-IV-resistant GLP-1 receptor agonist (incretin mimetic) exenatide (Byetta™) and the DPP-

IV inhibitor sitagliptin (Januvia™). Both have been shown to profoundly improve glucose homeostasis in type 2 diabetes (T2DM) (17-19).

There have been relatively few studies on the potential for incretin mimetics or DPP-IV inhibitors in the treatment of T1DM. Infusion or subcutaneous GLP-1 lowered fasting hyperglycemia and reduced glycemic excursions and requirements for exogenous insulin in T1DM patients (20, 21). In preclinical studies, the DPP-IV-inhibitor isoleucine thiazolidide improved glucose tolerance in both streptozotocin (STZ)-induced (22, 23) and BioBreeding (BB) (23) diabetic rats, with clear islet protection in the former group (22). The latter observation suggested that treatment with a DPP-IV inhibitor could also protect transplanted islets by increasing the endogenous levels of incretin hormones. In the present study, we examined the effect of administering the DPP-IV inhibitor sitagliptin on survival of islets transplanted under the kidney capsule of STZ-induced diabetic mice. Islet survival was assessed from fasting plasma glucose, intraperitoneal glucose tolerance tests (IPGTT) and positron emission tomography (PET) imaging.

EXPERIMENTAL PROCEDURES

Mice. Male C57BL/6 mice (10-12 week old) were obtained from the University of British Columbia (UBC) Animal Care Facility and the Jackson Laboratory (Bar Harbor, Maine). After 3-5 days acclimation, the animals received a single dose of STZ (200 mg/kg). One week after STZ treatment, the mice were placed on either a normal chow diet (NCD, Purina Rodent Chow #5015) or diet containing sitagliptin (24) (Purina Rodent Chow # 5015 plus 4 g MK0431 /Kg, Research Diets Inc., New Brunswick, NJ) *ad libitum*. All animal experiments were conducted in accordance with the guidelines put forth by

the University of British Columbia Committee on Animal Care and the Canadian Council on Animal Care.

DPP-IV activity assays. To measure the plasma DPP-IV activity, a fluorometric assay was employed using Gly-Pro-AMC, which is cleaved by the enzyme to release the fluorescent aminomethylcoumarin (AMC). A typical reaction contained purified DPP-IV enzyme for standard reaction or plasma sample, 50 μ M Gly-Pro-AMC and 100 mM Tris buffer, pH 8.0. Liberation of AMC was monitored using an excitation wavelength of 360 nm and an emission wavelength of 460 nm.

Measurement of total pancreatic insulin content. Pancreata were homogenized in 5 ml of ice-cold 2 N acetic acid, boiled and centrifuged (10 min, 15,000 rpm, 4°C). The insulin concentration in neutralized supernatants was determined by a radioimmunoassay (RIA; Linco Research Inc.) and normalized for protein concentration (BCA; Pierce, Rockford, IL).

Islet isolation and cell culture. Male C57BL/6 mice (10-12 week old) were anesthetized by intraperitoneal injection of pentobarbital (30-40 mg/kg) and islets isolated by collagenase digestion, followed by filtration through a 70 μ m nylon mesh cell strainer (25). Islets were hand-picked and cultured for 1-2 h prior to adenoviral infection in RPMI 1640 (Sigma) supplemented with 5.5 mM glucose, 0.25 % HEPES, 10 % fetal bovine serum, 100 units/ml penicillin G-sodium and 100 μ g/ml streptomycin sulfate (Invitrogen).

Generation of recombinant adenoviruses and islet gene transfer. Recombinant adenovirus expressing *HSV1-Sr39TK* was produced, expanded by infection of human embryonic kidney (HEK)-293 cells and multiplicity of infection (m.o.i.) determined by plaque assays (26). Islets were exposed to 250 m.o.i. of purified recombinant adenoviruses for 2 h at 37 °C and washed

three times with Hanks' Balanced Salt Solution (HBSS). Islets were then re-cultured for 16-24 h in RPMI 1640 medium (Sigma) supplemented with 5.5 mM glucose, 0.25 % HEPES, 10 % fetal bovine serum, 100 units/ml penicillin G-sodium and 100 μ g/ml streptomycin sulfate (Invitrogen) until transplanted or assayed for *in vitro* studies.

Islet transplantation. STZ (200 mg/kg) was intraperitoneally injected into C57BL/6 mice (male, 10-12 week old) 5 d before transplantation, and the mice with blood glucose levels \geq 20 mmol/l for three consecutive days were considered as diabetic. Under general anesthesia, induced by isoflurane inhalation, a lombotomy was performed, and kidneys exposed. A breach was made in the kidney capsule, and a polyethylene catheter was introduced through the breach and advanced in the subcapsular space to the opposite pole of the kidney. For all experiments 300 islets (not islet equivalents), obtained from C57BL/6 mice and infected with 250 m.o.i. of rAD-TK, were slowly injected and allowed to spread at the pole. The catheter was then retrieved, the opening cauterized and the kidney repositioned, followed by suturing of muscle and skin. Mice were allowed to regain consciousness and placed on either a NCD diet (Purina Rodent Chow #5015) or diet containing sitagliptin (24) (Purina Rodent Chow # 5015 plus 4 g MK0431 /Kg *ad libitum*).

Plasma glucose determinations, intraperitoneal glucose tolerance tests (IPGTTs) and plasma hormone measurements. Non-fasting blood glucose levels were measured in mouse-tail blood using a SureStep Glucose analyzer (LifeScan) at the time points indicated in Figures 2, 3 and 4. For the IPGTTs, mice were fasted for 4 h and blood glucose levels measured at 0, 15, 30, 60, 90 and 120 min following the glucose challenge (2 g/kg). Blood samples with glucose levels \geq 27.8 mmol/l were diluted

with blood from non-diabetic mice and levels calculated. Plasma insulin, glucagon and active GLP-1 levels were determined using a Multiplex assay kit (Linco Research Inc.).

Synthesis of 9-(4-[¹⁸F]-Fluoro-3-hydroxymethylbutyl)-guanine ([¹⁸F]FHBG). [¹⁸F]FHBG was synthesized by a modification of the method of Ponde *et al.* as previously described (27).

MicroPET scanning. Transplanted mice were scanned (27, 28) on day 1 (1st week) and days 8 (2nd week), 15 (3rd week), 22 (4th week) after the transplantation using a FocusTM 120 (CTI Concorde) system that yield 95 slices, 1.2 mm apart with an in plane resolution of 1.4 mm full-width at half-maximum (FWHM) (29) The mice were transported to the PET suite in their home cage. Shortly before scanning, they were anesthetized by isoflurane inhalation, placed on the scanner bed in a prone position and a nose cone was fitted over the face to maintain isoflurane anesthesia throughout the procedure. An intravenous catheter (27 G) was placed in the tail vein and saline was slowly dripped to maintain catheter patency. [¹⁸F]FHBG (100 μ Ci in 0.5 mL) was injected as a bolus in the tail vein. Scanning in list mode started upon tracer injection and lasted for 1 h.

Image reconstruction and data analysis. The data were subsequently framed and reconstructed with filtered back projection (FBP). In addition, to improve organ identification and the accuracy of positioning regions of interest (ROI), a single time frame from 30-60 min post injection was reconstructed using the three-dimensional iterative maximum *a posteriori* (MAP) algorithm (30), which yields images of higher resolution (31). Activity in the kidney area was usually visualized in 3-4 slices. The same pixel sizes of circular ROIs were drawn on the target areas on the 2 best slices of the MAP image containing the kidneys, to reduce the influence of partial volume effects. The ROIs were then repositioned on the

kinetically reconstructed data and time activity curves (TACs) were obtained for each region. The counts/pixel/minute obtained from the ROI were converted to counts/ml/minute by using a calibration constant obtained from scanning a cylinder phantom in the microPET scanner. The ROI counts/ml/minute were converted to counts/g/minute, assuming a tissue density of 1g/ml, and divided by the injected dose to obtain an image ROI-derived percentage injected dose of [¹⁸F]FHBG retained in kidney.

Statistical analysis. Data are expressed as means \pm Standard Errors of the Mean (SEM) with the number of individual experiments presented in the figure legends. Data were analyzed using the linear regression analysis program PRISM (GraphPad, San Diego, CA) and area under the curves (AUCs) were calculated using the algorithm provided in the Prism software package. Significance was tested using analysis of variance (ANOVA) with Newman-Keuls hoc test ($P < 0.05$) as indicated in figure legends.

RESULTS

Effects of orally administered MK0431 in STZ-induced diabetic mice. In previous studies it was shown that DPP-IV inhibitor treatment reduced the progressive severity of diabetes induced by STZ in the rat (22). In the single, high dose STZ-induced diabetic mouse model used for the islet transplant studies, a higher level of β -cell ablation was expected. However, to establish that significant islet protection or growth would not occur, MK0431 was administered in the chow (4 g/Kg) 1 week after STZ treatment, and the progression of diabetes studied. Plasma DPP-IV activity increased within the first week following STZ treatment. However, activity was greatly inhibited in the MK0431-treated mice, whereas plasma DPP-IV activity in mice receiving the standard diet continued to rise to levels that were \sim 250 % greater

(Figure 1A). Plasma levels of active GLP-1 were significantly increased in the diabetic mice treated with MK0431, demonstrating protection of circulating incretins from degradation (Figure 1B).

As expected, food intake was enhanced in the STZ-induced diabetic mice but in animals switched to chow containing MK0431, food intake decreased to levels similar to those prior to STZ treatment (Supplementary Figure 1A). Despite the lower food intake with the MK0431 diet, there were no significant differences in body weight between the two groups throughout the study, with an initial decrease and little change after the first week (Supplementary Figure 1B). Water intake increased to similar levels in both groups (Supplementary Figure 1C). MK0431 treatment had no significant effect on the highly elevated non-fasting blood glucose levels throughout (Figure 2A). At the end of the 5 week test period, mean fasting glucose, IPGTT blood glucose responses (Figures 2B, C & 2D), total pancreatic insulin content (Figure 2E) and plasma insulin/glucagon ratios (Figure 2F) did not differ between the MK0431 and NCD fed mice. Very few β -cells could be identified in histological sections of the pancreata (Data not shown). MK0431 treatment also resulted in no significant changes in fasting or non-fasting blood glucose levels or IPGTT blood glucose responses in non-diabetic control mice (Supplementary Figure 2 A-D).

MK0431 treatment improves islet graft survival in STZ-induced diabetic mice. The effect of MK0431 on islet graft survival was next studied. Prior to transplantation under the kidney capsule, islets were infected with a recombinant adenovirus expressing *HSV1-Sr39TK*, the gene for a mutant form of herpes simplex virus 1 thymidine kinase (rAD-TK) to allow PET imaging. It was previously determined that 250 m.o.i. was an appropriate dose for the treatment with rAD-TK, based on the level of Sr39TK expression, insulin

secretory capacity and islet cell viability (28). At 48 h after infection with 250 m.o.i. rAD-TK, $27 \pm 5 \%$ ($n=3$) of β -cells were positively stained for TK (Supplementary Figure 3). The number of islets used for transplantation (300) was chosen so as to partially correct the hyperglycemia in STZ-treated C57BL/6 mice for a limited period (32). For the first 1.5 weeks following transplantation both groups had similar body weights (Figure 3A) and water intake (Figure 3B). At this time, the MK0431 diet group began to gain body weight, whereas the NCD group did not, and water intake in the latter group increased profoundly. Three days following transplantation, non-fasting blood glucose levels were normalized in the MK0431 diet group, whereas levels in the non-treated mice progressively increased from 1.5 weeks on (Figure 3C). A similar trend was evident for fasting blood glucose (Figure 3D). During the course of the study, ~40% of the mice placed on NCD died, probably as a result of the severe hyperglycemia, whereas all of the mice on the MK0431 diet survived (Figure 3E). Following islet transplantation food intake decreased. This was followed by a progressive rise in food consumption in the NCD group to pre-surgery levels (Figure 3F). However food intake in the MK0431 group was significantly lower than the NCD group from week 2 onward (Figure 3F). Plasma DPP-IV activity was reduced by 78~88 % in the MK0431 group (Figure 3G) and plasma active GLP-1 levels were increased ~ 2.5-fold compared to the NCD group (Figure 3H). Although not reaching statistical significance, DPP-IV activity in the NCD group activity showed a downward trend from 1 week following transplantation (Figure 3G). There was no significant correlation between plasma DPP-IV activity and body weight, food consumption, water intake or blood glucose levels.

Intraperitoneal glucose tolerance tests (IPGTTs) were performed on both groups of mice at 1st, 2nd, 3rd and 4th week following transplantation ($n = 5$ animals/group). As expected, IPGTTs showed that transplanted islets in the NCD group lost their capacity to regulate blood glucose levels over time, because of the suboptimal dose of islets. By contrast, the MK0431 group preserved their capacity to regulate blood glucose levels normally until the end of the study (Figure 4). Basal plasma insulin in the NCD group was lower than in the MK0431 treated mice. Glucose-stimulated insulin secretion (GSIS) decreased greatly in the NCD group over the 4 weeks following transplantation, whereas the MK0431 group showed stable insulin secretory responses to glucose stimulation throughout (Figure 5A). While plasma glucagon levels increased substantially in the NCD group over the 3 weeks following transplantation, glucagon in the MK0431 group remained low (Figure 5B). As a consequence, plasma insulin/glucagon ratios were drastically decreased in the NCD group, whereas the MK0431 group showed constant ratios throughout, reflecting the control of blood glucose levels (Figure 5C). Together these results strongly suggested that MK0431 had positive effects on the regulation of hyperglycemia, potentially through prolongation of islet graft survival.

Assessment of functional islet mass in STZ-induced diabetic mice following islet transplantation. The effect of MK0431 on islet graft survival was determined by microPET imaging. Mutant thymidine kinase expressed in the transplanted islets phosphorylates the substrate [¹⁸F]FHBG following systemic injection, thus trapping it in intact cells. As previously demonstrated (27, 28), islet graft survival can then be quantified by PET scanning. The PET signal from transplanted islets in the NCD group decreased dramatically over time following transplantation. However, the MK0431 group

showed sustained PET signals for up to 4 weeks following transplantation (Figure 6). Histological staining of kidney sections confirmed islet graft preservation in the MK0431 group at 1 month following transplantation (data not shown). PET signal intensity from the mice with differing glucose tolerance correlated well with area under the curve (AUC) and GSIS ($R^2 = 0.86$ for AUC and $R^2 = 0.89$ for GSIS, Figures 7A and 7B), as well as slightly lower correlation with plasma glucagon levels ($R^2 = 0.81$) and the plasma insulin/glucagon ratio ($R^2 = 0.74$) (Figures 7C and 7D).

DISCUSSION

Multiple factors contribute to post-transplant islet loss (5-7), among which apoptosis is thought to play a major role. The incretin hormones GIP and GLP-1 both stimulate proliferation of β -cells while inhibiting apoptosis (8-12). Increasing the concentration of active incretins, by inhibiting their degradation with DPP-IV inhibitors, has been shown to be associated with β -cell preservation in animal models of T2DM (33). Additionally, in earlier studies it was shown that long-term (7-week) treatment of STZ-diabetic rats with the DPP-IV inhibitor, isoleucine thiazolidide resulted in reduced blood glucose levels and increases in pancreatic insulin content and the number of small islets (22), suggesting that DPP-IV inhibition could preserve islets *in vivo* and potentially prolong islet engraftment following transplantation.

The first study was performed to establish whether similar protective effects of DPP-IV inhibition would occur in the STZ-induced diabetic mouse model used for islet transplantation. Unexpectedly, treatment of mice with STZ resulted in a rapid increase in the levels of circulating DPP-IV. The reason for this is uncertain, but both the kidneys and liver express high levels of DPP-IV (34) as well as GLUT-2 (35), the transporter

responsible for uptake of STZ into cells. It is therefore possible that hepatic and/or renal damage was responsible for the sustained elevation of DPP-IV activity in the control mice. Increased release of DPP-IV from the endothelium or circulating lymphocytes may also have contributed to the increase in activity. Additionally, in other animal models of T1DM, we have also observed elevated levels of circulating DPP-IV activity, suggesting that hyperglycemia and/or hypoinsulinemia may play a role. Nevertheless, MK0431 treatment resulted in a marked reduction in the DPP-IV activity and enhanced active GLP-1 levels (Figures 1A and 1B). However, there were no significant effects of MK0431 on body weight, water intake (Supplementary Figure 1B and 1C) or fasting and non-fasting blood glucose levels (Figures 2A and 2B). Additionally, blood glucose responses during the 120-min course of IPGTT in diabetic mice were unchanged by the MK0431 diet (Figure 2C and 2D). The lack of a beneficial effect of the DPP-IV inhibitor is probably due to the low number of residual β -cells with the STZ treatment protocol utilized. The total pancreatic insulin content in the STZ-diabetic mice was only 7.3 ± 0.4 ng/mg protein, less than 30 % of that measured in the STZ rat pancreas (22) and β -cells were undetectable by histology.

In order to examine the potential protective effect of DPP-IV inhibitor treatment on transplanted islets, suboptimal doses of islets were transplanted in the STZ-diabetic mice. Although there is considerable variation in the number of islets reported to achieve euglycemia among different studies, we and others (32), have found that 300 islets is generally sub-optimal for C57BL/6 mice, resulting in transplanted mice that are very sensitive to the effects of treatments that either prolong or decrease islet graft survival. In pilot studies, mice that received transplants of lower numbers of islets (100) remained

hyperglycemic and did not benefit from treatment with MK0431 (data not shown).

The body weight in MK0431-fed mice increased by 4 g. over the study period, whereas the NCD mice lost weight. Non-fasted blood glucose levels in NCD-fed mice were decreased by ~ 15 mmol/l at 3 days following the islet transplantation, but levels increased to >30 mmol/l by 4 weeks (Figure 3C). Fasting blood glucose followed a similar trend (Figure 3D), reflecting the sub-optimal nature of the islet transplantation. By contrast, fasting and non-fasting blood glucose in islet transplanted diabetic mice on the MK0431 diet decreased below 10 mmol/l and remained so throughout the study period (Figures 3C and 3D). Intraperitoneal glucose tolerance tests (IPGTTs) confirmed that the transplanted islets in the NCD-fed group lost their capacity to regulate blood glucose levels over time (Figure 4), whereas the MK0431 group showed preserved ability to regulate blood glucose levels until the end of the study, with sustained GSIS and plasma insulin/glucagon ratios (Figure 4 and 5), suggesting prolongation of islet graft survival. The overall improvement in metabolic status of the MK0431-treated mice was also reflected in the stable water intake (Figure 3B) and much lower food consumption than the NCD-fed mice (Figure 3F), accompanied by the increase in body weight of the former group.

Although the metabolic studies indicated that MK0431 promoted islet survival, it was not possible to unambiguously discriminate between maintenance of islet mass and improved islet function. Although high correlations between metabolic determinations and independent measures of β -cell function have been obtained (36), assessment of functional islet mass through imaging can directly provide quantitative information on islet graft status. Additionally, such techniques are directly applicable for preclinical studies on drugs with the potential

for improving graft survival. Magnetic resonance imaging (MRI), optical imaging and PET all offer their own advantages. PET is a non-invasive metabolic imaging modality that has been extensively used to study biochemical and biological process *in vivo*. With the PET reporter gene (PRG)/PET reporter probe (PRP) system, based on a mutant form of herpes simplex virus 1 thymidine kinase (*HSV1-sr39tk*), the the PET signal is directly proportional to the enzymatic activity of sr39TK (37-38). Recently we (27-28), and others (39-40), showed that microPET imaging is directly applicable to the quantification of islet transplants. In the present study, the effect of MK0431 on functional islet mass was quantified by PET imaging throughout the 4-weeks, and there was a profound prolongation of the PET signal in the inhibitor-treated mice (Figure 6). PET signal intensity also showed a strong correlation with AUC or GSIS in the

IPGTTs (Figure 7), indicating that oral administration of MK0431 exerted cytoprotective effects on the transplanted islets.

In conclusion, the DPP-IV inhibitor MK0431, acting at least partially through increasing the circulating concentrations of active incretin hormones exerted protective effects resulting in the prolongation of islet graft survival.

ACKNOWLEDGEMENTS

These studies were generously supported by funding to CHSMc from Merck Frosst, Canada. We would like to thank Dr. Thomas J Ruth, Salma Jivan and TRIUMF for support and the preparation of [¹⁸F]FHBG, Siobhan McCormick for excellent technical assistance, and Dr. M. E. Black (Washington State University, WA, USA) for α -HSV1-Sr39TK antibody.

REFERENCES

1. Shapiro AMJ, Lakey JR, Ryan EA, Korbitt GS, Toth E, Warnock GL, Kneteman NM, Rajotte RV: Islet transplantation in seven patients with type 1 diabetes mellitus using a glucocorticoid-free immunosuppressive regimen. *New Eng. J. Med.* 343: 230-238, 2000.
2. Collaborative Islet Transplant Registry Annual Reports [<https://web.emmes.com/study/isl/reports/reports.htm>] (accessed 20 December 2007)
3. Ryan EA, Paty BW, Senior PA, Bigam D, Alfadhli E, Kneteman NM, Lakey JR, Shapiro AMJ: Five-year follow-up after clinical islet transplantation. *Diabetes* 54:2060-2069, 2005.
4. Boker A, Rothenberg L, Hernandez C, Kenyon NS, Ricordi C, Alejandro, R: Human islet transplantation: Update. *World J. Surg.* 25: 481-486, 2001.
5. Robertson RP: Editorial: Intrahepatically transplanted islets-Strangers in a strange land. *Endocrinology* 8: 5416-5417, 2002.
6. Davalli AM, Scaglia L, Zangen DH, Hollister J, Bonner-Weir S, Weir GC: Vulnerability of islets in the immediate posttransplantation period: dynamic changes in structure and function. *Diabetes* 45: 1161-1167, 1996.
7. Narang AS, Mahato RI: Biological and biomaterial approaches for improved islet transplantation. *Pharmacological Reviews* 58:194-243, 2006.
8. Brubaker PL, Drucker DJ: Minireview: Glucagon-like peptides regulate cell proliferation and apoptosis in the pancreas, gut, and central nervous system. *Endocrinology* 145: 2653-2659, 2004.
9. Drucker DJ. The biology of incretin hormones. *Cell Metab.* 3:153-165, 2006.
10. Ehses JA, Casilla VR, Doty T, Pospisilik JA, Winter KD, Demuth HU, Pederson RA, McIntosh CHS: Glucose-dependent insulinotropic polypeptide promotes beta-(INS-1) cell survival via cyclic adenosine monophosphate-mediated caspase-3 inhibition and regulation of p38 mitogen-activated protein kinase. *Endocrinology* 144: 4433-4445, 2003.
11. Kim SJ, Winter K, Nian C, Tsuneoka M, Koda Y, McIntosh CHS: Glucose-dependent insulinotropic polypeptide (GIP) stimulation of pancreatic beta-cell survival is dependent upon phosphatidylinositol 3-kinase (PI3K)/protein kinase B (PKB) signaling, inactivation of the forkhead transcription factor Foxo1, and down-regulation of bax expression. *J. Biol. Chem.* 280: 22297-22307, 2005.
12. Kim SJ, Nian C, Widenmaier S, McIntosh CHS: Glucose-dependent Insulinotropic Polypeptide (GIP) mediated up-regulation of β -cell anti-apoptotic *Bcl-2* gene expression is coordinated by cAMP-response element binding protein (CREB) and cAMP-responsive CREB coactivator 2 (TORC2). *Mol Cell Biol* 28:1644-1656, 2008.
13. Mentlein R, Gallwitz B, Schmidt WE: Dipeptidyl-peptidase IV hydrolyses gastric inhibitory polypeptide, glucagon-like peptide-1(7-36)amide, peptide histidine methionine and is responsible for their degradation in human serum. *Eur J Biochem* 214: 829-835, 1993.
14. Kieffer TJ, McIntosh CHS, Pederson RA: Degradation of glucose-dependent insulinotropic polypeptide and truncated glucagon-like peptide 1 in vitro and in vivo by dipeptidyl peptidase IV. *Endocrinology* 136: 3585-3596, 1995.
15. Deacon CF, Johnsen AH, Holst JJ: Degradation of glucagon-like peptide-1 by human plasma in vitro yields an N-terminally truncated peptide that is a major endogenous metabolite in vivo. *J Clin Endocrinol Metab* 80: 952-957, 1995.

16. Lambeir AM, Durinx C, Scharpe S, De Meester I: Dipeptidyl-peptidase IV from bench to bedside: an update on structural properties, functions, and clinical aspects of the enzyme DPP IV. *Crit Rev Clin Lab Sc*, 40: 209-294, 2003.
17. McIntosh CHS, Demuth H.-U, Kim SJ, Pospisilik JA, Pederson RA: Applications of dipeptidyl peptidase IV inhibitors in diabetes mellitus. *Int J Biochem Cell Biol* 38: 860-872, 2006.
18. Ahrén B: Dipeptidyl peptidase-4 inhibitors: clinical data and clinical implications. *Diabetes Care*. 30:1344-1350, 2007.
19. Drucker DJ, Nauck MA: The incretin system: glucagon-like peptide-1 receptor agonists and dipeptidyl peptidase-4 inhibitors in type 2 diabetes. *Lancet*. 368: 1696-1705, 2006.
20. Creutzfeldt WO, Kleine N, Willms B, Ørskov C, Holst JJ, Nauck MA: Glucagonostatic actions and reduction of fasting hyperglycemia by exogenous glucagon-like peptide I (7-36) amide in type I diabetic patients. *Diabetes Care* 19: 580-585, 1996.
21. Dupre J: Glycaemic effects of incretins in Type 1 diabetes mellitus: a concise review, with emphasis on studies in humans. *Regul Pept* 128:149-157, 2005.
22. Pospisilik JA, Martin J, Doty T, Ehses JA, Pamir N, Lynn FC, Piteau S, Demuth H.-U, McIntosh CHS, Pederson RA: Dipeptidyl peptidase IV inhibitor treatment stimulates beta-cell survival and islet neogenesis in streptozotocin-induced diabetic rats. *Diabetes* 52: 741-750, 2003.
23. Pospisilik JA, Ehses JA, Doty T, McIntosh CHS, Demuth H.-U, Pederson RA: Dipeptidyl peptidase IV inhibition in animal models of diabetes. *Adv Exp Med Biol* 524: 281-291, 2003.
24. Kim D, Wang L, Beconi M, Eiermann GJ, Fisher MH, He H, Hickey GJ, Kowalchick JE, Leiting B, Lyons K, Marsilio F, McCann ME, Patel RA, Petrov A, Scapin G, Patel SB, Roy RS, Wu JK, Wyvratt MJ, Zhang BB, Zhu L, Thornberry NA, Weber AE: (2R)-4-oxo-4-[3-(trifluoromethyl)-5,6-dihydro[1,2,4]triazolo[4,3-a]pyrazin-7(8H)-yl]-1-(2,4,5-trifluorophenyl)butan-2-amine: a potent, orally active dipeptidyl peptidase IV inhibitor for the treatment of type 2 diabetes. *J. Med. Chem.* 48: 141–151, 2005.
25. Salvalaggio PR, Deng S, Ariyan CE, Millet I, Zawalich WS, Basadonna GP, Rothstein DM: Islet filtration: a simple and rapid new purification. *Transplantation* 74: 877-879, 2002.
26. Becker TC, Noel RJ, Coats WS, Gómez-Foix AM, Alam T, Gerard RD, Newgard CB: Use of recombinant adenovirus for metabolic engineering of mammalian cells. *Methods Cell. Biol.* 43: 161-189, 1994.
27. Kim SJ, Doudet DJ, Studenov AR, Ruth TJ, Gambhir SS, McIntosh CHS: Seeing is believing – *In vivo* functional real-time imaging of transplanted islets using positron emission tomography (PET). *Nature Protocols Network*. http://www.natureprotocols.com/2006/12/21/seeing_is_believing_in_vivo_fu.php
DOI: 10.1038/nprot.2006.491.
28. Kim SJ, Doudet DJ, Studenov AR, Ruth TJ, Gambhir SS, McIntosh C.H.S: Quantitative in vivo imaging of transplanted islets using microPET (positron emission tomography) scanning. *Nature Med* 12: 1423-1428, 2006.
29. Kim JS, Lee JS, Im KC, Kim SJ, Kim SY, Lee DS, Moon DH: Performance Measurement of the microPET Focus 120 Scanner. *J. Nuc. Med.* 48: 1527-1535, 2007.
30. Qi J, Leahy RM, Hsu C, Farquhar TH, Cherry SR: Fully 3D Bayesian image reconstruction for the ECAT EXACT HR⁺. *IEEE Trans. Nucl. Sci.* 45: 1096–1103, 1998.

31. Chatziioannou A, Qi J, Moore A, Annala A, Nguyen K, Leahy R, Cherry SR: Comparison of 3-D maximum *a posteriori* and filtered back projection algorithms for high-resolution animal imaging with microPET. *IEEE Trans. Med. Imag.* 19: 507–512, 2000.
32. Richards SK, Parton LE, Leclerc I, Rutter GA, Smith RM: Over-expression of AMP-activated protein kinase impairs pancreatic β -cell function in vivo. *J. Endocrinol.* 187: 225-235, 2005.
33. Mu J, Woods J, Zhou Y-P, Roy RS, Li Z, Zycband E, Feng Y, Zhu L, Li C, Howard AD, Moller DE, Thornberry NA, Zhang B: Chronic inhibition of dipeptidyl peptidase-4 with a sitagliptin analog preserves pancreatic β -cell mass and function in a rodent model of type 2 diabetes. *Diabetes* 55:1695-1704, 2006.
34. Demuth H-U, McIntosh CHS, Pederson RA: Type 2 diabetes-therapy with dipeptidyl peptidase IV inhibitors. *Biochim Biophys Acta* 1751: 33-44, 2005.
35. Dufrane D, van Steenberghe M, Guiot Y, Goebbels R-M, Sakiez A, Gianello P: Streptozotocin-induced diabetes in large animals (pigs/primates): Role of GLUT2 transporter and β -cell plasticity. *Transplantation* 81: 36-45, 2006.
36. Robertson RP: Estimation of β -cell mass by metabolic tests. Necessary, but how sufficient? *Diabetes* 56: 2420-2424, 2007.
37. Yu Y, Annala AJ, Barrio JR, Toyokuni T, Satyamurthy N, Namavari M, Cherry SR, Phelps ME, Herschman HR, Gambhir SS: Quantification of target gene expression by imaging reporter gene expression in living animals. *Nature Med.* 6: 933-937, 2000.
38. Gambhir SS, Bauer E, Black ME, Liang Q, Kokoris MS, Barrio JR, Iyer M, Namavari M, Phelps ME, Herschman HR: A mutant herpes simplex virus type 1 thymidine kinase reporter gene shows improved sensitivity for imaging reporter gene expression with positron emission tomography. *Proc. Natl. Acad. Sci. USA* 97: 2785-2790, 2000.
39. Lu Y, Dang H, Middleton B, Zhang Z, Washburn L, Stout DB, Campbell-Thompson M, Atkinson MA, Phelps M, Gambhir SS, Tian J, Kaufman DL: Noninvasive imaging of islet grafts using positron-emission tomography. *Proc. Natl. Acad. Sci. USA* 103:11294-11299, 2006.
40. Lu Y, Dang H, Middleton B, Campbell-Thompson M, Atkinson MA, Gambhir SS, Tian J, Kaufman DL: Long-term monitoring of transplanted islets using positron emission tomography. *Mol Ther* 14:851-856, 2006.

FIGURE LEGENDS

Figure 1. MK0431 inhibits plasma DPP-IV activity and increases plasma active GLP-1 levels in STZ-diabetic mice. C57BL/6 mice treated with a single high dose of STZ (200 mg/kg) were placed on either a normal chow diet (NCD) or diet containing MK0431 (4g/kg). (A) Plasma DPP-IV activity and (B) plasma active GLP-1 levels 1 month after initiation of the MK0431 treatment. Number of animals: $n = 6$ per group: diabetic control (open rectangle) and diabetic control with MK0431 diet (filled rectangle). All data represent the mean \pm S.E.M. and significance was tested using ANOVA with a Newman-Keuls post hoc test, where ** represents $p < 0.05$ vs Diabetic.

Figure 2. The effects of MK0431 on glycemic control in STZ-diabetic mice. (A) Non-fasting and (B) fasting blood glucose levels, (C) and (D) intraperitoneal glucose tolerance tests (IPGTTs) and area under the curve (AUC), (E) total pancreatic insulin content and (F) plasma glucagon/insulin ratios were determined in the mice described in the legend Figure 1. Number of animals: $n = 6$ per each group: diabetic control (open rectangle) and diabetic control with MK0431 diet (filled rectangle). All data represent the mean \pm S.E.M. and significance was tested using ANOVA with a Newman-Keuls post hoc test, where *N.S.* represents not significant.

Figure 3. The effects of MK0431 on transplanted islets. Islets isolated from non-diabetic C57BL/6 mice were infected with 250 m.o.i. of rAD-TK, 300 of which were transplanted under the right kidney capsule of STZ-induced diabetic C57BL/6 mice. Following islet transplantation, mice were placed on either a normal chow diet (NCD, open circle) or MK0431 diet (filled circle). (A) Body weight (B) water intake, (C) non-fasting and (D) fasting blood glucose levels, (E) survival rate, (F) food consumption, (G) plasma DPP-IV activity and (H) plasma active GLP-1 levels following islet transplantation. Number of animals: $n = 5$ per group. All data represent the mean \pm S.E.M. and significance was tested using ANOVA with a Newman-Keuls post hoc test, where ** represents $p < 0.05$ vs NCD mice.

Figure 4. Time-course monitoring of glucose responses following islet transplantation. On the indicated days following transplantation, IPGTTs were performed on the mice described in the legend to Figure 3, with blood glucose levels measured at 0, 15, 30, 60, 90 and 120 min following the glucose challenge (2 g/kg): normal control mice (open triangle), mice placed on either NCD (open circle) and MK0431 diet (filled circle). Number of animals: $n = 3-5$ per group. All data represent the mean \pm S.E.M. and significance was tested using ANOVA with a Newman-Keuls post hoc test, where ** represents $p < 0.05$ vs normal control mice.

Figure 5. Time-course monitoring of plasma chemistry following islet transplantation. On the indicated days following transplantation, plasma insulin (A), glucagon (B) levels and plasma insulin/glucagon ratios (C) were determined in the mice described in the legend to Figure 4. Number of animals: $n = 5$ per group. All data represent the mean \pm S.E.M. and significance was tested using ANOVA with a Newman-Keuls post hoc test, where ## represents $p < 0.05$ vs basal at NCD mice, && represents $p < 0.05$ vs basal at MK0431 mice and ** represents $p < 0.05$ vs NCD mice.

Figure 6. Time-course monitoring of MicroPET signals detected from recipient diabetic mice following islet transplantation. Mice described in the legend to Figure 4 were injected with [¹⁸F]FHBG on the indicated days following transplantation and scanned. Regions of interests (ROIs) were placed on the kidney area of the microPET image and two peak values of % ID/g from the 2 time activity curves (TACs) for each region were used for determination of the signals. Number of animals: $n = 5$ per group. All data represent the mean \pm S.E.M. and significance was tested using ANOVA with a Newman-Keuls post hoc test, where ** represents $p < 0.05$ vs NCD mice.

Figure 7. Correlation between PET signals and metabolic tests. Correlation between PET signals and (A) area under the curve (AUC), (B) Glucose stimulated insulin secretion (GSIS), (C) Plasma glucagon levels and (D) Plasma insulin/glucagon ratios. Data were analyzed using the linear regression analysis program PRISM.

Figure 1.

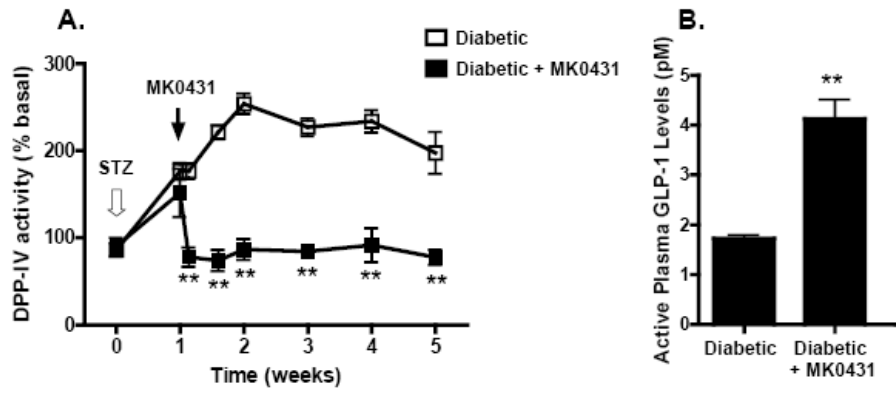


Figure 2.

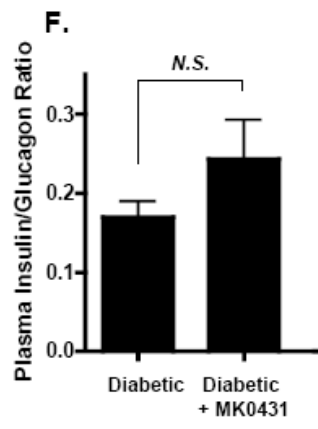
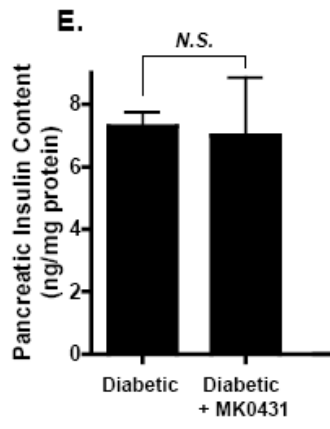


Figure 3.

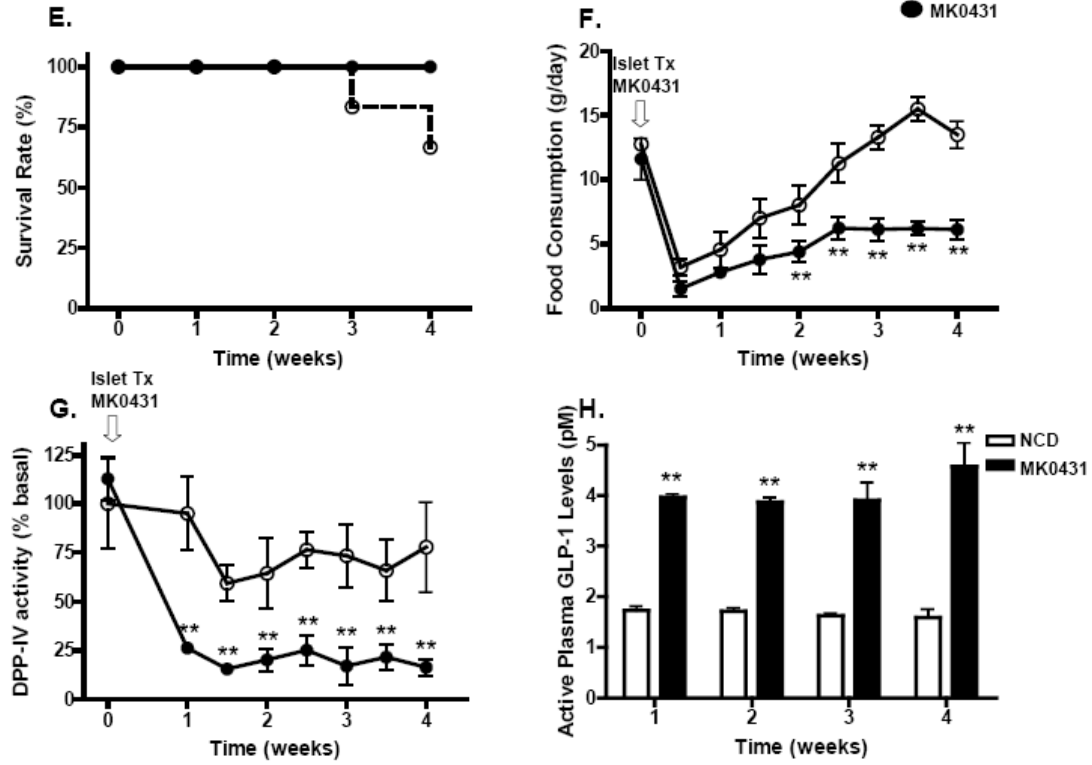


Figure 4.

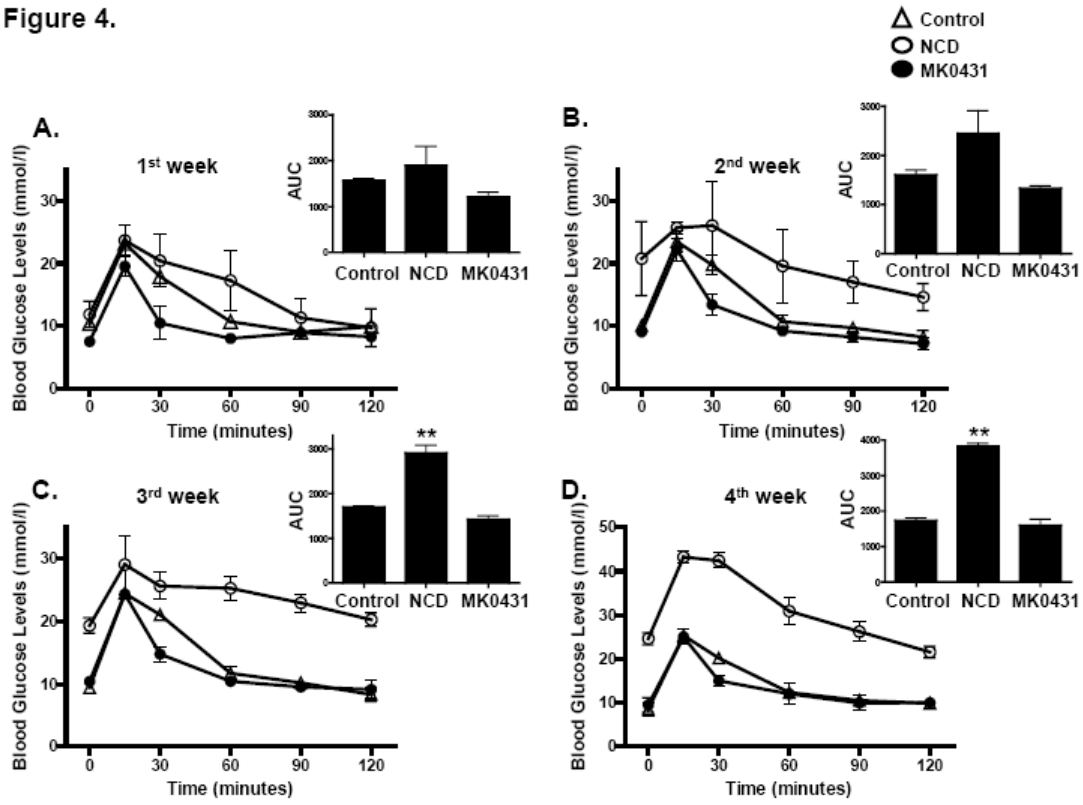


Figure 5.

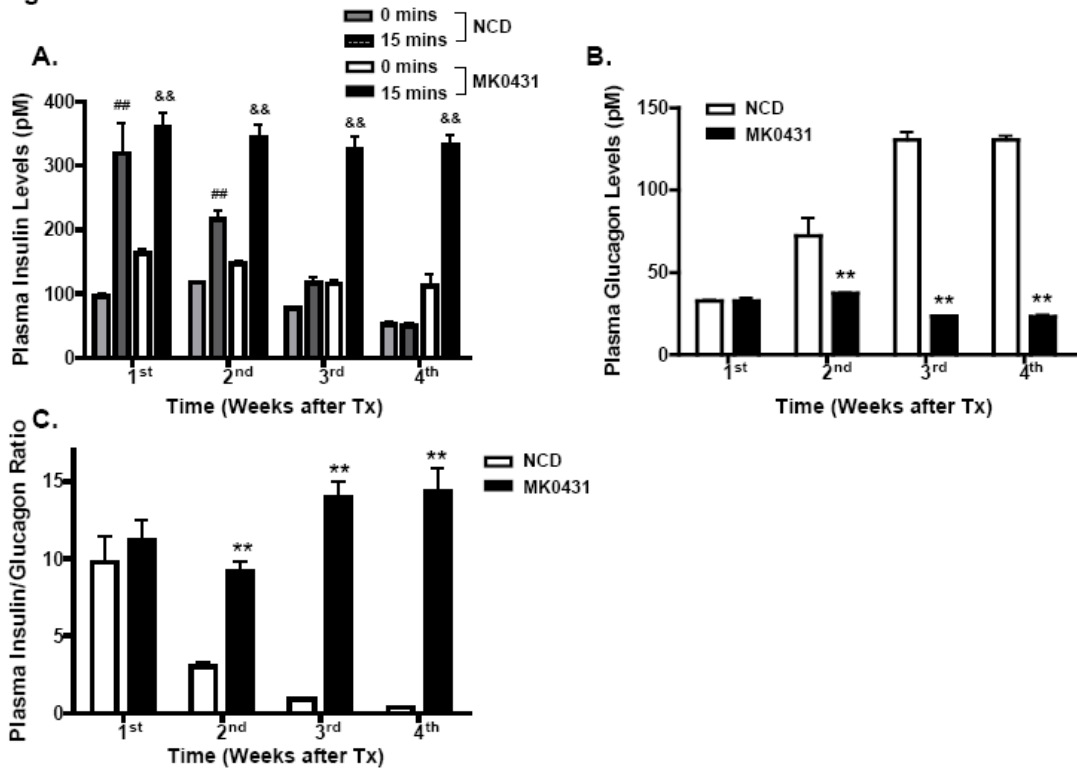


Figure 6.

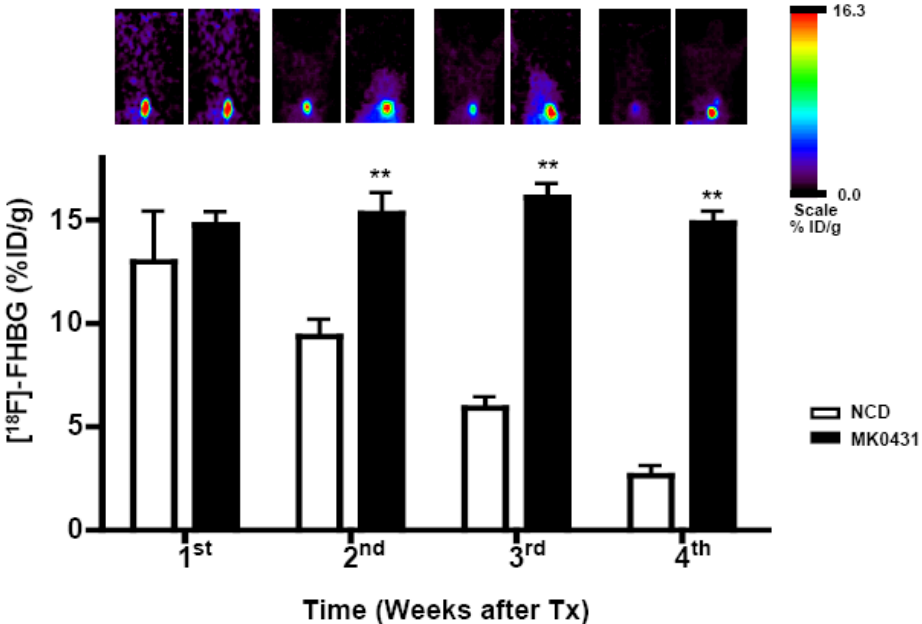


Figure 7.

